

# Progress in the Construction of the 43 T Hybrid Magnet at LNCMI-Grenoble

P. Pugnat, R. Barbier, C. Berriaud, R. Berthier, T. Boujet, F. Debray, P. Fazilleau, P. Graffin, P. Hanoux, B. Hervieu, F. Molinié, H. Neyrial, M. Pelloux, C. Peroni, R. Pfister, Y. Queinec, L. Ronayette, and B. Vincent

(Invited Paper)

**Abstract**—By combining resistive polyhelix and Bitter insert coils with a large bore superconducting outsert one, the new hybrid magnet in construction at LNCMI-Grenoble will produce in a first step, an overall continuous magnetic field of 43 T in a 34 mm warm bore aperture. After a brief reminder of the specificity of hybrid magnets, namely the strong electromagnetic and mechanical coupling between resistive and superconducting coils, the main specificities of the proposed design are presented. The superconducting coil of 1.1 m cold bore diameter will provide a nominal magnetic field of at least 8.5 T. It relies on the specific development of the Nb-Ti/Cu Rutherford cable on conduit conductor (RCOCC) cooled down to 1.8 K by a bath of superfluid helium at atmospheric pressure. The novelty of the RCOCC concerns the in-laboratory assembly with induction soft-soldering of the Rutherford cable on a Cu-Ag hollow stabilizer allowing a strict control of the quantity of the solder alloy used and therefore of the interstrand contact resistance. A stainless steel reinforced copper shield inserted between the superconducting and resistive coils will allow reducing the coupling currents induced within the RCOCC as well as the mechanical force exerted on the superconducting coil. After successful thorough reviews of the Grenoble hybrid magnet design anticipating possible upgrades of the maximum magnetic field produced, this project is now well engaged in its construction phase. The status of this project is presented in details together with the next milestones.

**Index Terms**— Hybrid magnet, large bore superconducting magnet, resistive magnet, superfluid helium, very high field magnet.

## I. INTRODUCTION

**H**YBRID MAGNETS combining superconducting and resistive technologies are still today the optimal solution

Manuscript received August 25<sup>th</sup>, 2017.

This project is supported by the CNRS, the French Ministry of Higher Education and Research in the framework of the “Investissements pour l’avenir” Equipex LaSUP (Large Superconducting User Platform), the European Funds for Regional Development (FEDER) and the Rhône-Alpes region.

P. Pugnat, R. Barbier, T. Boujet, F. Debray, P. Hanoux, M. Pelloux, C. Peroni, R. Pfister, L. Ronayette, and B. Vincent are with LNCMI, European Magnetic Field Laboratory (EMFL), CNRS-UGA-INSA-UPS, BP 166, 38042 Grenoble cedex-9, France (e-mail: Pierre.Pugnat@lncmi.cnrs.fr).

C. Berriaud, R. Berthier, P. Fazilleau, P. Graffin, B. Hervieu, F. Molinié, H. Neyrial, and Y. Queinec are with IRFU CEA-Saclay, 91191 Gif-sur-Yvette cedex, France.

for producing the highest continuous magnetic fields with limited electrical power consumption [1],[2]. High field hybrid magnets, *i.e.* producing at least 40 T, are of the very rare species with only two in operation worldwide [3],[4], and two others in construction including the LNCMI-Grenoble one [5],[6]. Their realization remains a technological challenge mainly due to difficulties in building the large external superconducting coil (SC) that shall survive not only quenches but also extreme electromechanical forces originating from its coupling to resistive inserts during fault operation modes [7].

The Grenoble hybrid magnet (Fig.1) is the only one offering to the scientific community a modular experimental platform with several high field and high flux magnet configurations ranging from 43 T in 34 mm to 9 T in 800 mm diameter, from the various combinations of superconducting and resistive coils [6],[8]. It proposes also some innovative developments with respect to other hybrid magnets based on the design proposed by the NHMFL in Tallahassee Florida relying on the Nb<sub>3</sub>Sn cable in conduit conductors (CICC) with a forced flow of supercritical He for the superconducting part [9] and on the Florida Bitter technology for the resistive one.

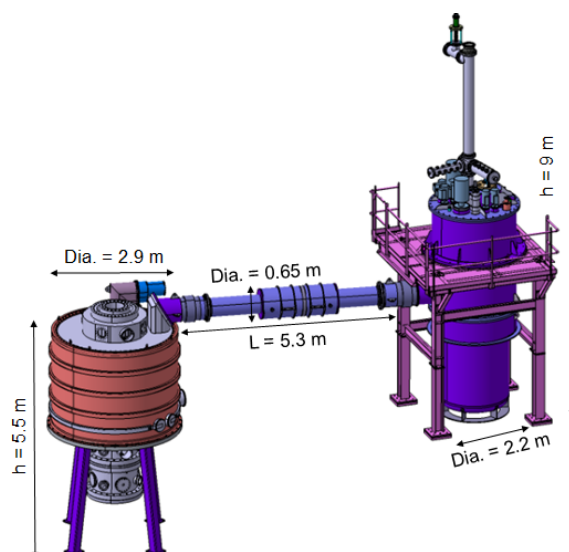


Fig. 1. 3D view of the Grenoble hybrid magnet (left side) connected via a cryogenic line to its cryogenic satellite producing the superfluid He.

The strategy for the Grenoble hybrid magnet design consists in pushing the resistive coils to their present limit whereas the superconducting outsert will be based on the most conservative and validated technology, *i.e.* Nb-Ti/Cu with pressurized superfluid He at 1.8 K, to produce at least 8.5 T. This cooling technology initially developed at Grenoble in the mid-70's allows to profit from the increase of the superconducting properties at low temperature without increasing the risk of electrical breakdown at fairly low voltages during the magnet operation [10].

In a first step, each of the two resistive coils of the hybrid magnet will be connected to a 12 MW power converter. The central polyhelix coil will produce 25.5 T and the surrounding two stack Bitter coils 9 T [6],[11] for a total maximum field of 43 T in a 34 mm warm bore aperture. The upgrade phase to exceed 45 T will be possible in a second step, thanks to the on-going upgrade of the electrical power installation from 24 up to 30 MW (phase 1) and then up to 36 MW (phase 2) [12]. The upgrade of the hybrid magnet has been anticipated in the design phase in both following directions: i) By using first a conservative worst case scenario for the dimensioning of mechanical structures [6],[13] and then by studying in details a more realistic one [7]. ii) By providing sufficient margin to the superconducting conductor to increase the field produced by the SC up to 9 T.

## II. RUTHERFORD CABLE-ON-CONDUIT CONDUCTOR

### A. Overview of the superconducting conductor

The Nb-Ti/Cu Rutherford cable on conduit conductor (RCOCC) is composed by a 19 strand flat cable soft-soldered on a hollow Cu-Ag stabilizer (Fig. 2) with final parameters listed in Table I, which can be compared to the design ones [14]. Such a conductor allows obtaining a cryostable SC internally cooled down to 1.8 K by a static bath of superfluid helium pressurized at 1200 mbar.



Fig. 2. Picture of the cross-section of the Rutherford cable on conduit conductor (RCOCC) produced. The dimensions are given in Table I.

The two main requirements for the RCOCC are: i) State-of-the-art soft-soldering of the Rutherford cable on the Cu-Ag hollow stabilizer; ii) Low inter-strand coupling currents to avoid premature quench of the superconducting magnet during a trip of the power converters of the resistive magnets. This later point constitutes one of the main novelties of the RCOCC and has driven specific developments to strictly control the adjacent contact resistance between strands and therefore the amount of the soft-solder alloy to use during the assembly. To increase the cross contact resistance of the RCOCC a stainless steel core of 50  $\mu\text{m}$  thickness was inserted within the Rutherford cable.

TABLE I  
AS BUILT MAIN PARAMETERS OF THE RCOCC (OVERALL PRODUCTION)

Parameters	Values(Max/min)
Width of the non-insulated RCOCC <sup>a</sup>	12.96 $\pm$ 0.04 mm
Height of the non-insulated RCOCC <sup>a</sup>	17.92 $\pm$ 0.05 mm
Copper cross-section of the Cu-Ag stabilizer	$\geq$ 157.4 mm <sup>2</sup>
Cross-section of the cooling channel	$\geq$ 28.3 mm <sup>2</sup>
Proof stress at 0.2% after soldering 300 K / 4.2 K	> 230 / 290 MPa
RRR of the stabilizer after the soft-soldering	65 $\pm$ 5
Twist pitch of the Rutherford cable ( $L_p$ )	$\leq$ 140 $\pm$ 5 mm
Strand diameter before cabling	1.62 $\pm$ 0.02 mm
Strand coating thickness	3 $\mu\text{m}$ of SnAg <sub>5wt%</sub>
Cross/adjacent contact resistances $R_c/R_a$ <sup>b</sup>	> 100 / > 0.5 $\mu\Omega$
Strand Cu/Nb-Ti ratio	1.24 $\pm$ 0.06
Filament diameter / twist pitch	14 $\mu\text{m}$ / 15 $\pm$ 1 mm
$I_c$ of the RCOCC at T = 1.9 K & B = 10 T <sup>c</sup>	> 20 610 A
Unit length	265 m

<sup>a</sup>From continuous measurement control during the production on straight RCOCC prior to its winding in single pancake of 2 m internal diameter in its delivery spool.

<sup>b</sup>Effective contact resistance  $R_a$  deduced from thermometry measurements at 4.2 K [14] on samples extracted from the production; it is an effective value as it includes the heating coming from the interfilamentary contributions.

<sup>c</sup>Deduced from measurements on strands; this value corresponds to a margin on the peak field load line of about 22% as well as a temperature margin of 2.4 K at nominal current and peak field equal to 9.35 T.

### B. Production of the Nb-Ti/Cu Rutherford Cable

A total length of about 13 km of flat Rutherford cable with 19 strands of 1.6 mm diameter assembled around the stainless steel foil of 50  $\mu\text{m}$  of thickness was successfully produced and delivered by Bruker EAS GmbH in December 2012. Most of the difficulties were encountered during the cabling process at Furukawa Co, Ltd to achieve a mechanically stable cable with dimensional tolerances of the width and thickness of  $\pm 0.04$  mm and  $\pm 0.03$  mm, respectively (max/min of the whole production). For this, a strict control of the dimensions of the flat Rutherford cable with a dedicated cable measuring machine was introduced on the cabling line and cross-checked with similar measurements performed at CERN [14]. Critical currents ( $I_c$ ) have been measured on extracted strands in industry, at CERN as well as at LNCMI-Grenoble [14],[15]. Good agreements have been obtained between all these measurements. The  $I_c$  values are typically 5–18% larger than the specification of 315 A at 4.22 K and 9.5 T, with the index of the resistive transition  $n \approx 15$  and values of the ratio  $I_c(1.90 \text{ K}, 12.5 \text{ T})/I_c(4.22 \text{ K}, 9.5 \text{ T}) \approx 0.93\text{--}1.01$ .

### C. Production of the Cu-Ag hollow stabilizer

To prepare the industrial production of the hollow Cu-Ag stabilizer with tight geometrical tolerances in 325 m unit lengths, a specific R&D program has been realized in collaboration with Aurubis Belgium. The production of the hollow stabilizer consists of a continuous extrusion forming (CONFORM) followed by a cold drawing. Various full lengths of stabilizer in CuAg<sub>0.03-0.05%</sub> with the proper geometry and various hardening levels were produced and deeply characterized including chemical analysis, proof strength measurements at 300 K and 4.2 K, grain sizes characterization from optical microscope, hardening and micro-hardening

measurements as well as residual resistive ratio ( $RRR$ ) between 300 K and 4.2 K. The proof stress ( $\sigma_{p0,2\%}$ ) measured at 4.2 K (Table I) is significantly larger than the maximum Von Mises stress of 203 MPa calculated at 9 T central magnetic field from finite element modeling [16]. The addition of silver in the copper for the stabilizer follows a twofold objective, which was carefully checked: i) No significant decrease of  $\sigma_{p0,2\%}$  can be measured once the hollow stabilizer was submitted to thermal cycles reproducing the RCOCC soft-soldering (30 s at 230°C) as well as typical impregnation processes of the SC (9 h at 140°C) and ii) the average  $RRR$  value measured is limited to 65.

The reception tests of all  $\text{CuAg}_{0.04\%}$  stabilizer unit lengths were based on systematic dimensional measurements and leak test of the superfluid He channel (leak rate  $< 10^{-5}$  mbar l/s).

#### D. RCOCC industrial assembly in the laboratory

To obtain an average adjacent contact resistance between strands  $R_a > 0.5 \mu\Omega$  (Table I), the industrial process for the RCOCC assembly shall allow a strict control of the amount of soft-solder needed. As a consequence, the induction heating has been chosen to melt soft-solder ribbons instead of the melted solder bath usually used in industry. This approach also offers the advantage of reducing the environmental impact by minimizing the release of heavy metal vapors. Mechanical properties of soft-soldered RCOCC obtained from various ribbons of solder alloy have been thoroughly tested and analyzed leading to the final choice of  $\text{Sn}_{61.5}\text{Pb}_{37}\text{Sb}_{1.5}$  alloy [6] with a liquidus temperature of 190°C. The final thickness and width of the soft-solder ribbon used are equal to 0.11 mm and 14 mm, respectively.

No industrial partner was found for the production of the RCOCC mostly because this assembly was considered too risky for a standard tendering procedure. The only way to continue the project was to internalize such a production in the laboratory and place a call for tenders to build the production line. Thanks to a fruitful collaboration with Ravni Technologies, the industrial assembly line was delivered and installed at LNCMI-Grenoble first half of 2016.

The production line of the RCOCC can be split in 5 major parts: i) The unspooling drum of the Cu-Ag stabilizer and the straightening rollers. ii) The fluxing unit and the assembly head for the stabilizer, the soft-solder ribbon alloy and the flat Rutherford cable. iii) The open induction coil [6], the crimping head, the calibration one and the air cooling system. iv) The water cooling system, the ultrasonic control system to monitor the quality of the soft-soldering, the air dryer and the dimensional control system. v) The bending unit to form a single pancake coil of 2 m internal diameter for the RCOCC delivery in unit length of 265 m; it can be emphasized that the minimal bending radius is larger than the maximum one of the final double pancake coil winding.

#### E. RCOCC verification tests

During the production of the RCOCC, the ultrasonic signal to control the quality of the soft-soldering was recorded continuously as well as both dimension measurements

(Table I). A sample of 2 m long was extracted from each produced length of RCOCC for thorough quality control tests and measurements. This allowed affirming that no degradation of the mechanical and electrical properties of the RCOCC components have been introduced during the assembly, soft-soldering and dimensional calibration processes. Ultimate shear stress between the Rutherford cable and the Cu-Ag stabilizer has also been measured on the extracted samples in the range 24–37 MPa at room temperature and the adjacent contact resistance  $R_a \approx 0.5\text{--}0.6 \mu\Omega$  at 4.2 K (Table I).

The production of all RCOCC unit lengths was completed end of July 2017 and delivered to the coil manufacturer. This milestone can be considered as one the first great achievements of the project.

### III. SUPERCONDUCTING COIL DESIGN AND MANUFACTURING

#### A. Design overview

The main parameters of the SC are given in Table II and a 3D section view is shown Fig. 3.

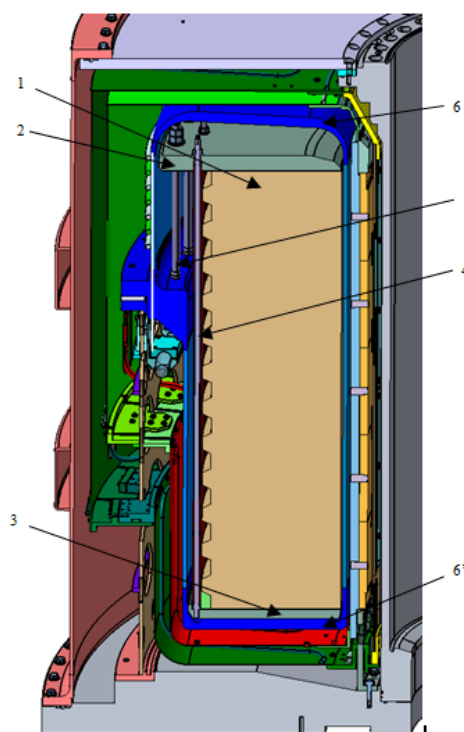


Fig. 3. 3D section view of the superconducting coil (SC) within its cryostat. The SC (1) is fitted between the upper (2) and the lower plates (3), which are connected together with the coil tie rods (4) during the assembly for the handling and transport. A pre-stress is applied between the upper plate (2) and the bottom part of the helium (He) vessel (6') with additional tie rods (5). The He vessel consists of two welded parts, the upper (6) and the bottom (6') ones enclosing the SC. It is surrounded by the vacuum vessel of the SC cryostat.

The SC winding is made of 37 double pancakes (DP) of  $2 \times 26$  layers each, electrically connected in series [6]. Each of them is obtained from the winding of 241 m long insulated RCOCC with its cooling channel of 6 mm diameter open in both ends to the static bath of pressurized superfluid He. During the industrial production each DP is vacuum

impregnated separately before being stacked, glued in a monolithic coil and electrically interconnected. In case of serious problem during the commissioning or the operation, the SC can be disassembled to replace the defective DP.

TABLE II  
UPDATED MAIN PARAMETERS OF THE SUPERCONDUCTING COIL

Parameters	Values
Inner / outer diameter	1106 / 1920 mm
Height	1406 mm
Coil weight	16.3 tons
Nominal / ultimate current (8.5 T / 9 T)	7115 / 7516 A
Resistance of each junction of the SC (x 36)	< 1 nΩ in 2 T
Inductance	3 H
Stored Energy (8.5 / 9 T)	76 / 84 MJ
Operating temperature	≤ 1.8 K

A two-step sorting strategy was implemented to optimize the performance of the SC alone in view of exceeding the maximum field of 9 T in 800 mm diameter. This magnet configuration is more dependent of the conductor performance compared to the hybrid ones as resistive insert coils lower the peak field in the SC. Firstly, Rutherford cable lengths with the highest  $I_c$  have been associated to Cu-Ag profile with the highest  $\sigma_{p0.2\%}$  during the RCOCC production. Secondly, these conductor lengths are used to produce “golden” DP that will be positioned in the mid-plane of the SC, whereas other DPs with progressive decreasing values of  $I_c$  and  $\sigma_{p0.2\%}$  will be pushed away in direction of both coil ends.

#### B. Status of the coil manufacturing

The contract for the coil manufacturing has been signed with Babcock Noell GmbH in January 2016 and one of the main difficulties encountered concerns the technical specification of the turn to turn adhesion, which shall hold a shear stress as high as 36 MPa at room temperature. Except this serious concern, the validations of the winding line and of the epoxy resin impregnation process are close to completion. Two dummy DP have been produced and cut for a thorough visual inspection. This allows defining and implementing several corrective actions such as:

- The increase of the interturn insulation from 2 ribbons half-overlap to three ones half-overlap as the compression of the fiber glass ribbons was higher than expected,
- The re-enforcement of the sandblasting to improve the bounding of the fiber glass ribbons on the RCOCC,
- The introduction of a RCOCC surface treatment with a coating layer of silane or another primer.

Recently, encouraging results have been obtained for the turn to turn bounding with ultimate shear stress reaching 38 and 33.5 MPa. These results still need to be consolidated and the series production of the DP will start hereafter. A total of 42 DP will be produced in addition to the 2 dummy ones whereas only 37 are required for the SC, leaving the possibility to get several spare DP in case of serious

damage(s) during at least 10 years of operation. The implications for such replacement have been anticipated since the design phase.

#### IV. CRYOSTAT AND MECHANICAL STRUCTURES

An overview of the cryostat of the overall system is given in Fig. 1. It is composed of three interconnected parts namely the cryostats of the SC, of the cryogenic line and of the satellite. The insulation vacuum has been segmented in two parts with a vacuum barrier in the middle of the 5.3 m long cryogenic line.

The cryostat of the SC has been designed for 1.8 K operation [17] and is composed of both a top and a bottom plates, an outer vacuum chamber, an inner bore tube containing the resistive electro-magnets at 300 K, the Eddy Current Shield (ECS) cooled down to 30 K, two sets of thermal screens at 50 K and 120 K and the helium vessel containing the SC (Fig. 3). The ECS was introduced to decrease the AC losses induced in the superconducting conductor during a sudden burn-out or trip of the resistive coils, *i.e.* fault operation mode requiring a slow discharge of the current, by reducing the flux variations to prevent a quench of the SC [18],[19]. It also protects the SC by reducing the applied maximum forces that can originate from a failure of resistive magnets [7]. Among innovative developments, the support ferrules for the ECS and the SC can be highlighted [6],[17]. The contracts for the manufacturing of the satellite and the cryostat of the SC have been signed with SDMS in April and December 2016, respectively.

#### V. CRYOGENICS

Cryogenics of the Grenoble hybrid magnet has already been presented [8], [17]. It can be split into two main parts.

##### A. Internal cryogenics

The internal cryogenics is dedicated to the production of the superfluid He and is based on the so-called Claudet bath [20], one of the main component of the cryogenic satellite (Fig. 1). It is worth emphasized that the pumping group to produce the superfluid pumped He has been oversized to allow reducing the temperature of the bath to 1.6 K leaving the possibility to further increase the maximum field produced by the SC. The cryogenic satellite also contains a 10 K reservoir of 1.5 m<sup>3</sup> dedicated to the recovery of about 60% of the liquid He during a quench, the remaining part being evaporated and evacuated through the relieve valve of the satellite.

##### B. External cryogenics

The external cryogenic infrastructure of the hybrid magnet is dedicated to the production and storage of liquid He starting from 200 bar He gas. It is mainly composed by a pumping system, a recovery system, and a 150 l/h helium liquefier connected to a buffer Dewar of 4500 liters. Due to budget constraints, all above equipment were purchased well in advance compared to the project schedule. Main parameters of the helium liquefaction system are given in Table III. The first phase of commissioning for the tests of the compressor started mid-November 2014 and lasted one month. The liquefier capacity has been measured a first time during 24 h in

February 2015. It reached 144 l/h at rising level in the Dewar at 1.3 bara with the internal purifier in operation, 0.1 % of He impurities and precooling with LN<sub>2</sub>. After further tests and a precise tuning of the purifier valves, the liquefier system reached finally in May 2015, 150 l/h in the same operating conditions as previously, which allowed its formal reception.

TABLE III  
 MAIN PARAMETERS OF THE HELIUM LIQUEFACTION SYSTEM

Air Liquide Helial ML liquefier parameters	Values
Liquid helium production with Grade-A He gas <sup>a</sup>	150 l/h <sup>b</sup>
Equivalent cooling power at 4.5 K	500 W <sup>b</sup>
Liquid Nitrogen precooling at 80K	90 l/h
Buffer volume for 170 m <sup>3</sup> NTP of pure He gas at 11.5 bar	15 m <sup>3</sup>
Compressor helium mass flow	55 g/s
NTP equivalent compressor helium volumetric flow	1200 m <sup>3</sup> /h
Compressor operating pressure	14.5 bar
Cooling water flow at 20°C (compressor and cold box)	14 m <sup>3</sup> /h
Electrical power consumption	192 kW

<sup>a</sup>Measured at rising level in the Dewar at 1.3 bar (15 % less if measured at constant level in the Dewar).

<sup>b</sup>With the internal cryogenic purifier in operation.

## VI. MAGNET CONTROL AND PROTECTION SYSTEMS

The aim of the Magnet Control System (MCS) is to control and monitor the cryogenics and the power supply of the superconducting magnet. The MCS is made of standard industrial products and is composed of a low level automation system for managing the process efficiently and a high level human machine interface for monitoring the parameters. The operation of the resistive coils is controlled via the LNCMI standard Magnet Control and Monitoring System (MCMS). The protection of the SC is insured by dedicated hardware systems named Magnet Safety Systems (MSS).

For the protection of the SC during a quench, the MSS sends the orders to open the circuit breakers CP1 and CP2 (Fig. 4) allowing the discharge of the stored energy of 76 MJ at nominal current, in dump resistors of 70 mΩ producing a maximum temperature and voltage across terminals of 60 K and 500 V, respectively [19]. A slow discharge mode is also foreseen in case of a defect requiring the limitation of the magnetic field decay such as for example in case of a trip of

the resistive inserts. In this case the management system (MCS/MSS) sends the orders to open CP1 and CP2 and to close CS3 or CS4 allowing the disconnection of the load from the converter and the decay of the current in the SC to compensate the induced current increase. The magnetic energy of the SC is discharged into one of the resistor SR or FR of 35 mΩ with a maximum voltage of 250 V and a time constant of 86.5 s. The redundant switch CS4 (Fig. 4) will be implemented at a later stage to improve the reliability of the slow discharge mode. When CS4 is closed after CS3, it also allows a strong reduction of the field decay and therefore of the induced currents in the SC, and this let the possibility of reconnecting the power converter when the normal operating temperature is reached.

The key elements to trigger the appropriate protective actions of the SC are the Magnet Safety Systems, which are duplicated for reliability issue in three independent modules. MSS-I is based on the voltage compensation method using mostly the voltage difference from 4 adjacent DP with a threshold for the quench detection, typically of 1 V during 1 s [19]. To insure the full redundancy of the SC protection, *i.e.* relying on different types of measurements, a cryogenic MSS or MSS-III based on temperature and pressure measurements for the quench detection is also being built. In addition, the possibility to install at a later stage MSS-II relying on new technology based on voltage measurements conversion and full numerical detection, is foreseen. This will also provide the opportunity of testing the reliability of new electrical magnet protection systems in noisy environment for future projects. An overview of the global architecture of MSS and MCS systems are given in Fig. 5 integrating the existing MCMS of resistive magnets. To manage the various configurations of the hybrid magnets a dedicated Hybrid Magnet Supervisor is being implemented.

Concerning the construction, most of the electronic cards for MSS-I as well as the acquisition systems for MSS-I, MSS-III and MCS have been ordered. The cabling and assemblies of all electronic components are well advanced and should be finalized first half of 2018.

The power converter with the energy extraction system has been delivered by Danfysik in August 2015 after being tested in industry up to 7500 A (stability and endurance tests). It has been further tested in 2016 at LNCMI using a more representative dummy load.

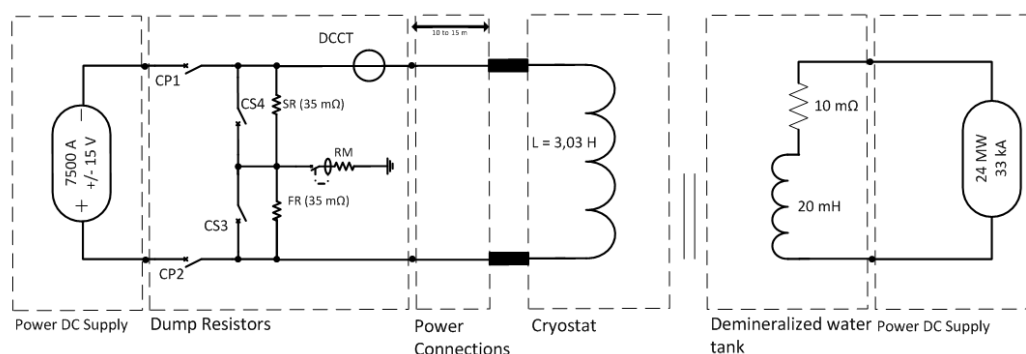


Fig. 4. Electrical scheme of the Grenoble hybrid magnet, including the superconducting and resistive coils connected to their power converters. Their mutual coupling is reduced by the eddy current shield. The resistive part has been (over)simplified into a single circuit whereas it is composed of the polyhelix and Bitter coils each being connected to a 12 MW power converter.

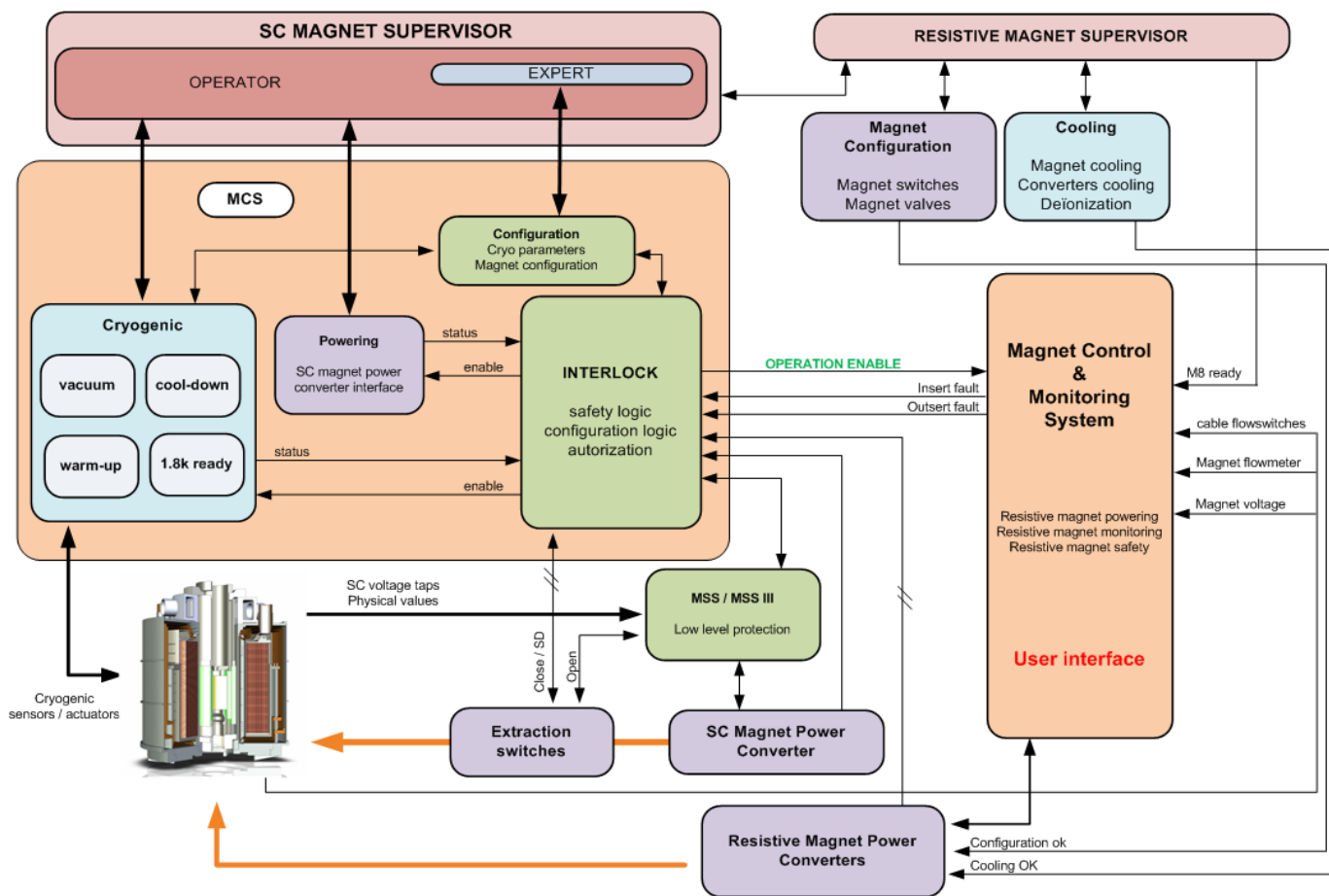


Fig. 5. Overview of the architecture integrating the control and protection systems of resistive and superconducting magnets. All the parts dedicated to the resistive magnets (right side) are already operational. They will be interfaced to the MSS, MCS and SC Magnet Supervisor under construction.

## VII. CONCLUSION

The main activities of the project are now focused on the supervision and follow-up of the last signed industrial contracts, which concern the construction and realization of the SC, the cryogenics satellite, the cryostat, the MSS and MCS. The call for tenders for the cryogenic line should be published in autumn 2017. All equipment should be delivered in 2018 at LNCMI-Grenoble for the final assembly. The cryogenic satellite will be first commissioned alone with the current leads in short-circuit prior to be interconnected to the magnet cryostat via the cryogenic line.

In parallel to these activities, experimental proposals are being studied exploiting the unique opportunities of this modular high field / high flux hybrid magnet platform. One of them plans to combine RF technologies and dilution cryostats in high field environment for axion and axion-like-particle dark matter searches with unprecedented sensitivities [21].

## ACKNOWLEDGMENT

The project team gratefully acknowledges the members of the technical advisory committee, namely Krzysztof Brodzinski (CERN), Alain Hervé (University of Wisconsin-Madison, chairman), Andries den Ouden (High Field Magnet

Laboratory, Radboud University), Hans J. Schneider-Muntau (Consultations Scientifiques et Techniques, CS&T), and Andrzej Siemko (CERN).

## REFERENCES

- [1] M. Wood and B. Montgomery, "Combined superconducting and conventional magnets," *Les Champs Magnetiques Intenses*, vol. 166 of *Colloques Internationaux du CNRS*, Grenoble, September 1966.
- [2] P. Pognat and H. J. Schneider-Muntau, "Hybrid Magnets: Past, Present and Future," *IEEE Trans. Appl. Supercond.*, vol. 24, no. 3, 4300106, 2014.
- [3] M. D. Bird, S. Bole, Y. M. Eyssa, B. J. Gao, and H. J. Schneider-Muntau, "Test results and potential for upgrade of the 45 T hybrid insert," *IEEE Trans. Appl. Supercond.*, vol. 10, no. 1, pp. 439–442, 2000.
- [4] G. Kuang, *et al.*, "The Hybrid Magnet at CHMFL," *IEEE Trans. Appl. Supercond.*, submitted for publication.
- [5] A. den Ouden, *et al.*, "Progress in the Development of the HFML 45 T Hybrid Magnet," *IEEE Trans. Appl. Supercond.*, vol. 26, no. 4, 4301807, 2016.
- [6] P. Pognat, *et al.*, "Status of the 43-T Hybrid Magnet of LNCMI-Grenoble," *IEEE Trans. Appl. Supercond.*, vol. 26, no. 4, 4302405, 2016.
- [7] H.J. Schneider-Muntau, *et al.*, "Ultimate Forces of the Grenoble Hybrid Magnet," *IEEE Trans. Appl. Supercond.*, submitted for publication.
- [8] L. Ronayette, *et al.*, "Cryogenic system for the 43 T Hybrid Magnet at LNCMI Grenoble: from the needs to the commissioning," *IOP Conf. Series: Materials Science and Engineering*, vol. 171, 012107, 2017.

- [9] M. D. Bird, "CICC Magnet Development at theNHMFL," *IEEE Trans. Appl. Superconduct.*, vol. 22, no. 3, 4300504, 2012.
- [10] G. Bon Mardion, G. Claudet and J.C. Vallier, "Superfluid helium bath for superconducting magnets," Proceedings of the 6<sup>th</sup> International Cryogenic Engineering Conference, Grenoble, pp. 159–162, 1976.
- [11] F. Debray, *et al.*, "DC High Field Magnets at theLNCMI," *IEEE Trans. Appl. Supercond.*, vol. 22, no. 3, 4301804, 2012.
- [12] R. Barbier, *et al.*, "Upgrade of the Grenoble High Magnetic Field Facility," *IEEE Trans. Appl. Supercond.*, submitted for publication.
- [13] P. Manil *et al.*, "Dynamical Response of Hybrid Magnet Structure Featuring Eddy-Current Shield During Transient Failure Mode", *IEEE Trans. Appl. Supercond.*, vol. 24, no. 3, 4300306, 2014.
- [14] P. Pagnat *et al.*, "Study and Development of the Superconducting Conductor for the Grenoble Hybrid Magnet," *IEEE Trans. Appl. Superconduct.*, vol. 22, no. 3, 6001604, 2012.
- [15] R. Pfister, W. Joss, S. Kraemer, P. Pagnat, L. Ronayette, and H. Xiao, "A New Test Station to Measure the Critical Current of Superconducting Strands," *IEEE Trans. Appl. Supercond.*, vol. 22, no. 3, 9500504, 2012.
- [16] C. Pes, C. Berriaud, P. Fazilleau, B. Hervieu, R. Pfister, M. Pissard, and P. Pagnat, "Two-Dimensional and Three-Dimensional Mechanical Analyses of the Superconducting Outsert of the LNCMI Hybrid Magnet," *IEEE Trans. Appl. Supercond.*, vol. 26, no. 4, 4301505, 2016.
- [17] B. Hervieu, *et al.*, "Cryogenic design of the 43 T LNCMI Grenoble Hybrid magnet," *Physics Procedia*, vol. 67, pp. 692–697, 2015.
- [18] A. Bonito Oliva *et al.*, "The 8-T 1.1 m bore superconducting solenoid for the 40 T hybrid magnet of the Grenoble High Magnetic Field Laboratory," *IEEE Trans. Appl. Supercond.*, vol. 10, no. 1, pp. 432–438, 2000.
- [19] P. Fazilleau, G. Aubert, C. Berriaud, B. Hervieu, and P. Pagnat, "Role and Impact of the Eddy Current Shield in the LNCMI-G Hybrid Magnet," *IEEE Trans. Appl. Supercond.*, vol. 26, no. 4, 4301305, 2016.
- [20] G. Claudet, A. Lacaze, P. Roubeau, and J. Verdier, "The design and operation of a refrigerator system using superfluid helium," Proceedings of the 5<sup>th</sup> International Cryogenic Engineering Conference, Kyoto, pp. 265–267, 1974.
- [21] P. Pagnat, *et al.*, "Preliminary Study for a New Axion Dark-Matter Haloscope," Proceedings of the 12<sup>th</sup> Patras Workshop on Axions, WIMPs and WISPs, Jeju Island (South Korea), 2016, to be published. <https://indico.desy.de/getFile.py/access?contribId=11&resId=0&materialId=slides&confId=13889>